Construction of neutral linear supramolecular polymer *via* orthogonal donor–acceptor interactions and pillar[5]arene-based molecular recognition

Panpan Chen, Julfikar Hassan Mondal, Yujuan Zhou, Huangtianzhi Zhu and Bingbing Shi*

Department of Chemistry, Zhejiang University, Hangzhou 310027, P. R. China.

Fax: +86-571-8795-3189; Tel: +86-571-8795-3189; Email address: bingbingshi@zju.edu.cn

Electronic Supplementary Information (18 pages)

1. Materials and methods

All reagents were commercially available and used as supplied without further purication. Copillar[5]arene **1a**[S1] and **2**[S2] were prepared according to the literature procedure. ^{1}H or ^{13}C NMR spectra were recorded with a Bruker Avance DMX 500 spectrophotometer or a Bruker Avance DMX 400 spectrophotometer with use of the deuterated solvent as the lock and the residual solvent or TMS as the internal reference. Viscosity measurements were carried out with a Cannon-Ubbelohde semi-micro dilution viscometer at 298K in chloroform. Scanning electron microscopy investigation was carried out on a JEOL 6390LV instrument. UV−Vis spectra were taken on a Perkin-Elmer Lambda 35 UV−Vis spectrophotometer. The fluorescence spectra were recorded on a Perkin Elmer LS55 fluorescence spectrophotometer.Low-resolution electrospray ionization mass spectra were recorded with a Bruker Esquire 3000 Plus spectrometer. High-resolution mass spectrometry experiments were performed with IonSpec 4.7 Tesla FTMS.

2. Synthesis and characterizations of compounds

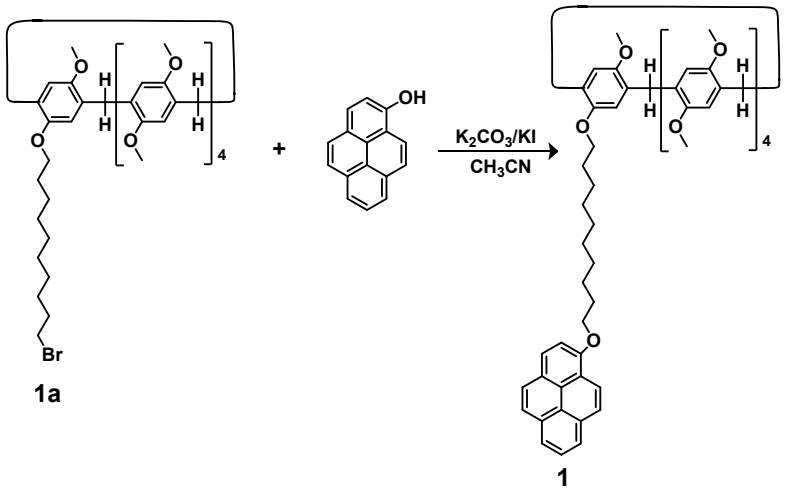

Scheme S1 *Synthetic route to* ***1***.

Copillar[5]arene **1a** was synthesized according to previous literature.[S1] In a 250 mL round–bottom flask, copillar[5]arene **1a** (1.20 g, 1.25 mmol), K_2CO_3 (1.55 g, 11.25 mmol), KI (0.08 g, 0.5 mmol), 1-Pyrenol (0.41 g, 1.88mmol) and acetonitrile (150ml) was added and the reaction mixture was stirred under N_2 for 48 h at 85 ^oC. After removal of the inorganic salt by filtration, the solvent was evaporated and the residue was dissolved in CH_2Cl_2. The resultant solution was washed with H_2O. The organic phase was collected and dried over anhydrous Na_2SO_4. The solvent was evaporated to provide a crude product, which was purified by column chromatography (eluent: petroleum ether/ethyl acetate, 10:1) to give **1** (1.17 g, 86.0 %) as a white solid. Mp: 76.5–77.2 ^oC. The proton NMR spectrum of **1** is shown in Fig. S1. ^1H NMR (400 MHz, $CDCl_3$, 298K) δ (ppm): 8.50 (d, J = 12 Hz, 1H), 8.13–8.03 (m, 4H), 7.98–7.94 (m, 2H), 7.90 (d, J = 12 Hz, 1H) 7.59 (d, J = 8 Hz, 1H), 6.85–6.79 (m, 10H), 4.11 (t, J = 12 Hz, 2H), 3.90 (t, J = 12 Hz, 2H), 3.79–3.77 (m, 10H), 3.69–3.65 (m, 27H), 1.81–1.76 (m, 2H), 1.61–1.49 (m, 8H), 1.37–1.24 (m, 6H). The ^{13}C NMR spectrum of **1** is shown in Fig. S2. The ^{13}C NMR (100 MHz, $CDCl_3$, 298K) δ (ppm): 152.28, 149.61, 149.56, 149.40, 148.81, 130.73, 130.67, 127.53, 127.25, 127.18, 127.14, 127.10, 126.23, 125.15, 125.04, 124.81, 124.48, 123.98, 123.81, 123.14, 123.03, 120.27, 119.27, 113.47, 112.95, 112.86, 112.83, 112.70, 112.64, 108.06, 67.99, 67.07, 54.80, 54.68, 54.65, 54.63, 54.52, 51.84, 28.60, 28.41, 28.26, 28.16, 28.11, 28.04, 28.01, 24.81, 24.70. LRESIMS is shown in Fig. S3: m/z 1110.8 [**1** + NH_4]$^+$; m/z

1115.7 [**1** + Na]$^+$. HRESIMS is shown in Fig. S4: *m*/*z* calcd for [**1** + NH_4]$^+$ $C_{70}O_{11}H_{80}N^+$, 1110.5889; found 1110.5707; error −16 ppm; *m*/*z* calcd for [**1** + Na]$^+$ $C_{70}O_{11}H_{76}Na^+$, 1115.5394; found 1115.5263; error −12 ppm.

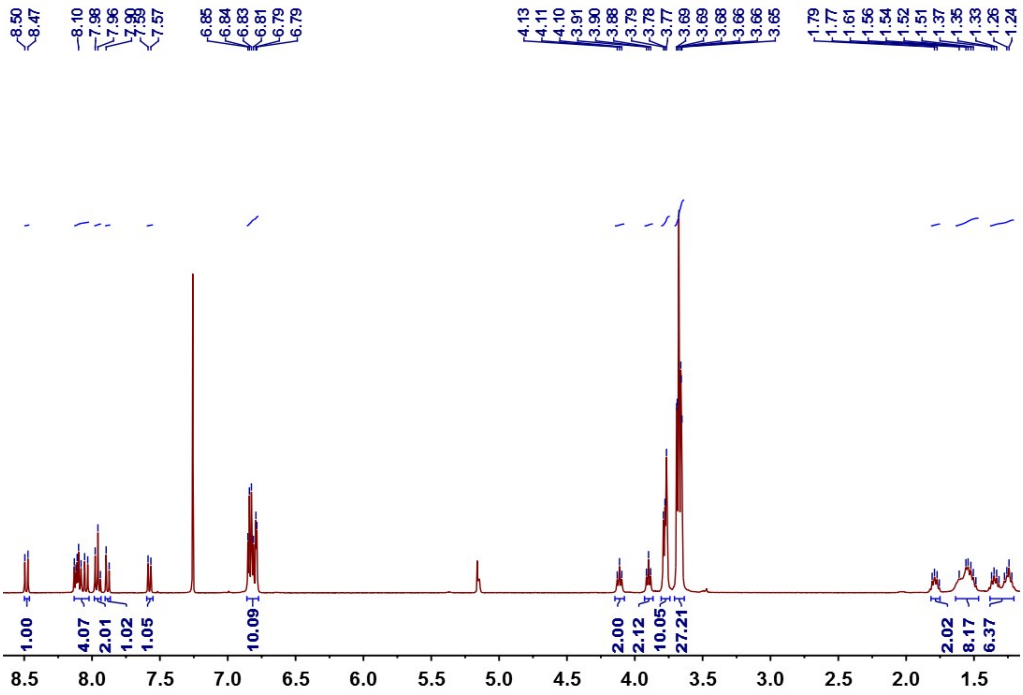

Fig. S1 ^{1}H NMR spectrum (400 MHz, $CDCl_3$, 298K) of pillar[5]arene **1**.

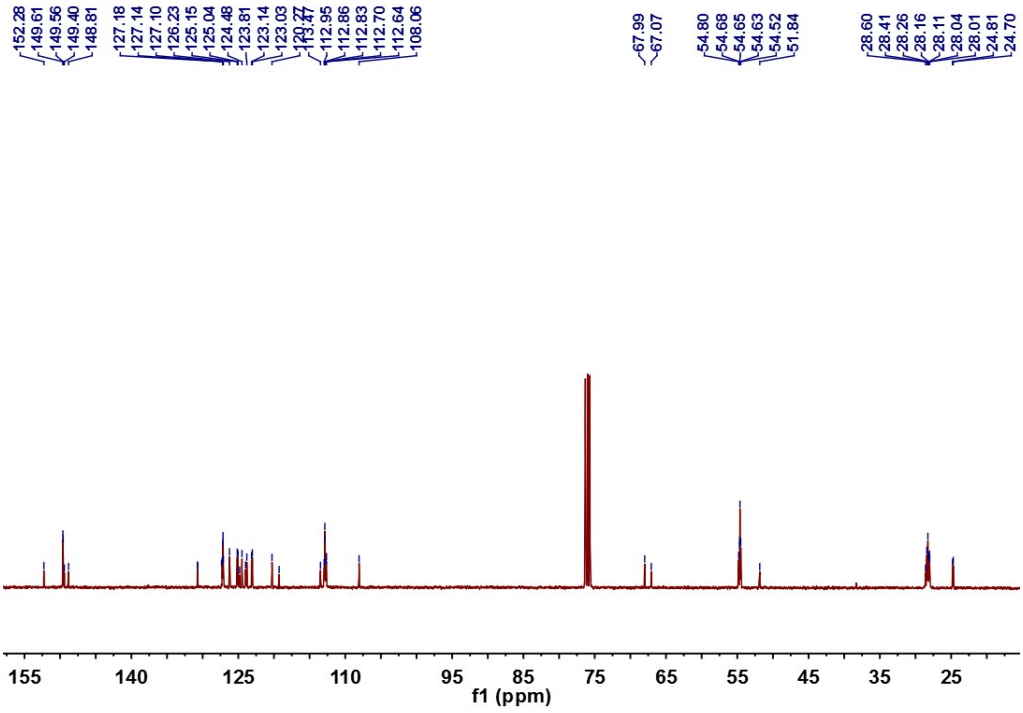

Fig. S2 ^{13}C NMR spectrum (100 MHz, $CDCl_3$, 298K) of pillar[5]arene **1**.

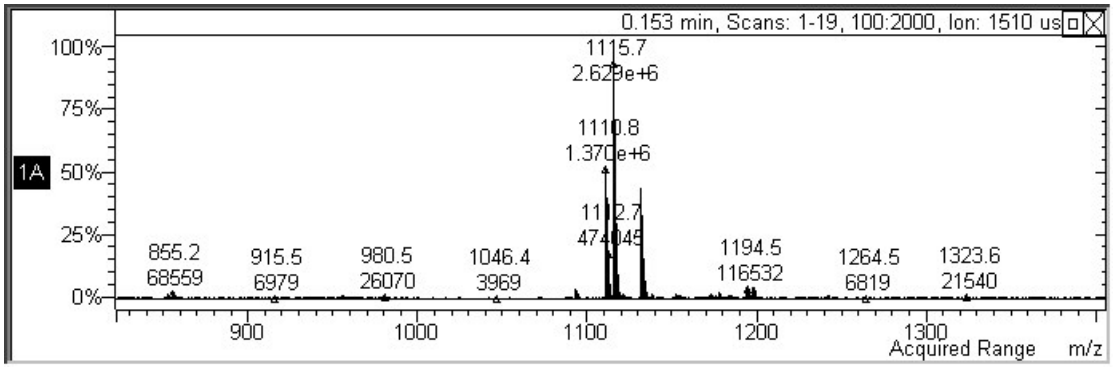

Fig. S3 ESI-MS spectrum of pillar[5]arene **1**.

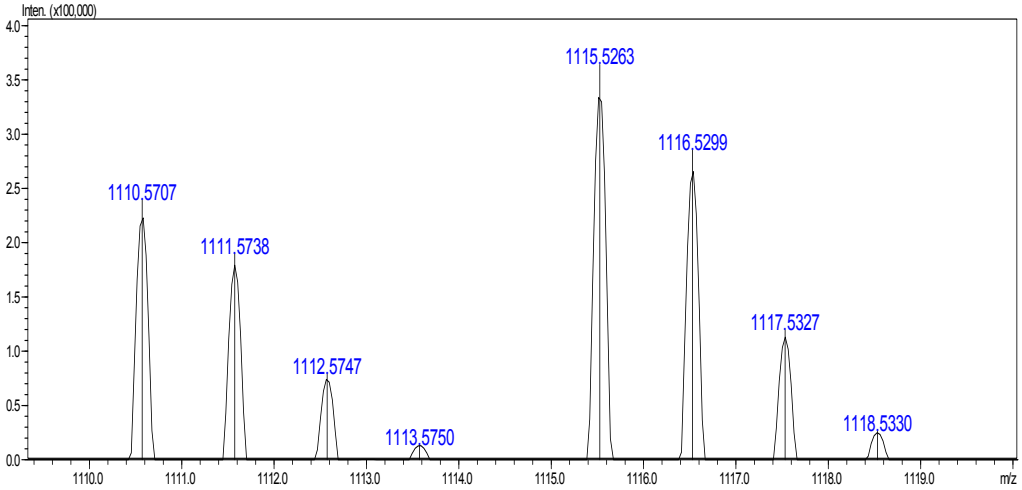

Fig. S4 High resolution electrospray ionization mass spectra of pillar[5]arene **1**.

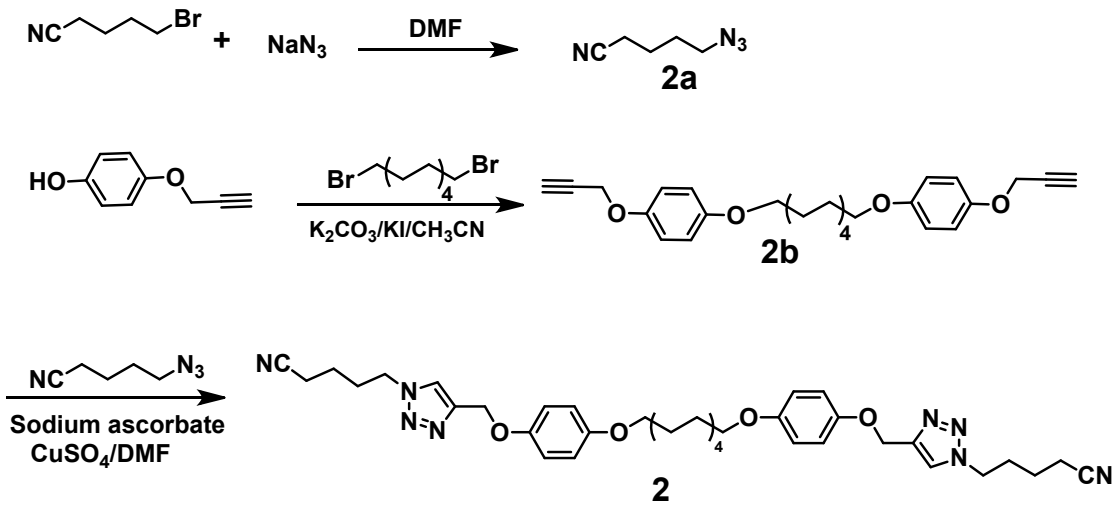

Scheme S2 *Synthetic route to neutral guest **2**.*

Neutral guest **2** was synthesized according to previous literature.[S2] ^{1}H NMR spectrum of **2a** is shown in Fig. S5. ^{1}H NMR (400 MHz, $CDCl_3$, 298K) δ (ppm): 1.75 (t, J = 4 Hz, 4H), 2.41 (t, J = 12 Hz, 2H), 3.37 (t, J = 12 Hz, 2H).

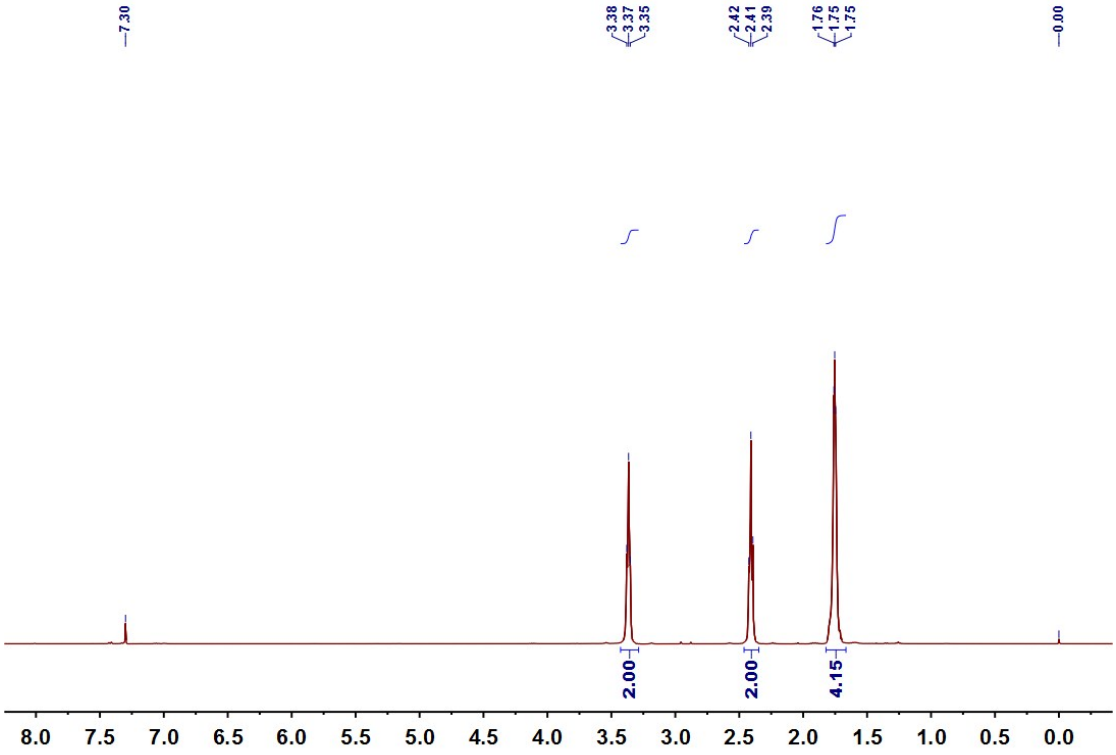

Fig. S5 ^{1}H NMR spectrum (400 MHz, $CDCl_3$, 298K) of **2a**.

The proton NMR spectrum of **2b** is shown in Fig. S6. ^{1}H NMR (400 MHz, $CDCl_3$, 298K) δ (ppm): 6.92 (d, J = 8 Hz, 4H), 6.84 (d, J = 8 Hz, 4H), 4.63 (s, 4H), 3.90 (t, J = 12 Hz, 4H), 2.50 (t, J = 8 Hz, 2H), 1.77–1.73 (m, 4H), 1.45–1.42 (m, 4H), 1.32 (m, 8H). The ^{13}C NMR spectrum of **2b** is shown in Fig. S7. The ^{13}C NMR (100 MHz, $CDCl_3$, 298K) δ (ppm): 154.05, 151.56, 116.10, 115.32, 78.96, 75.30, 68.54, 56.62, 29.51, 29.40, 29.37, 26.06.

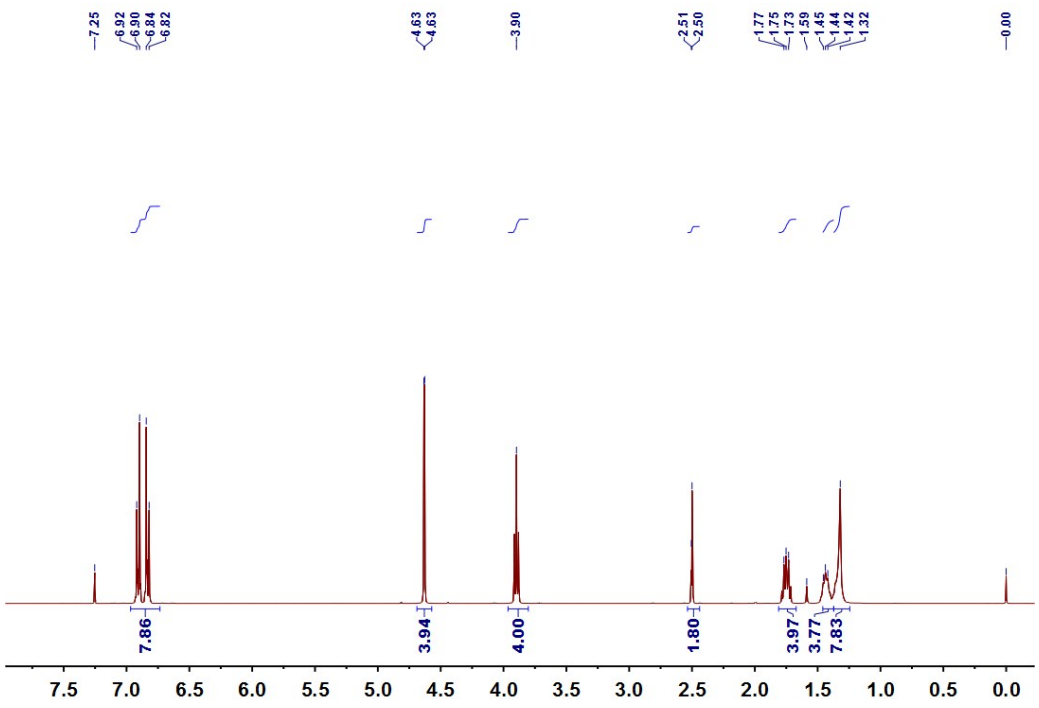

Fig. S6 ^{1}H NMR spectrum (400 MHz, $CDCl_3$, 298K) of **2b**.

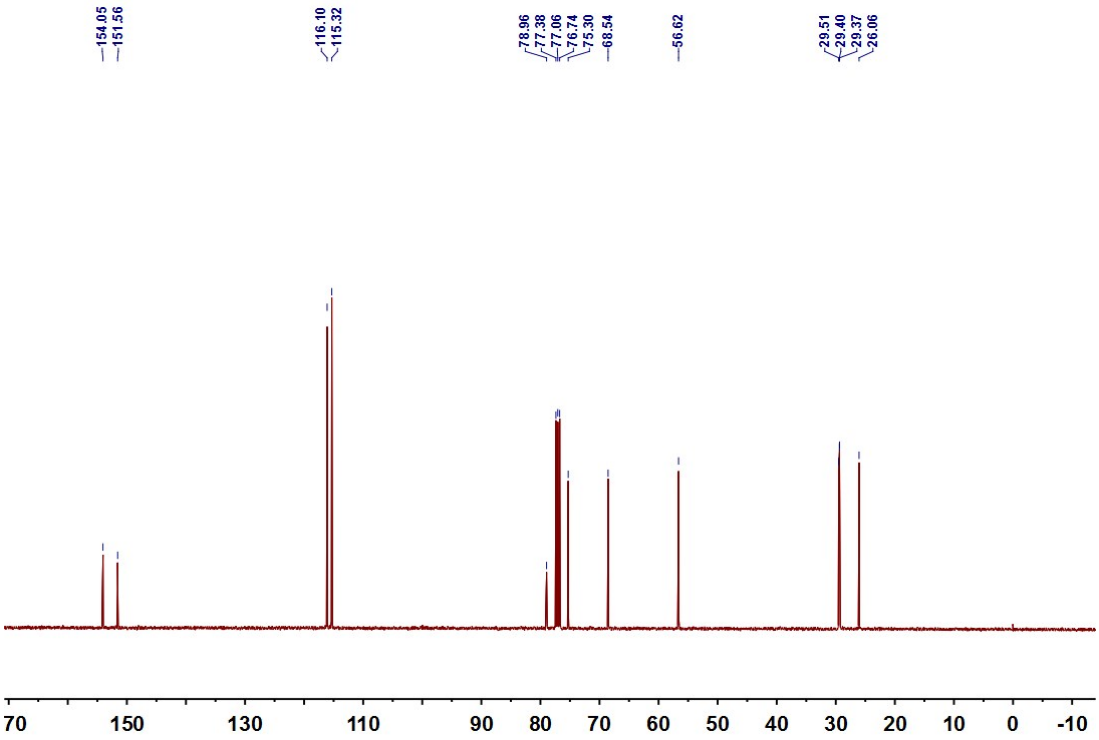

Fig. S7 ^{13}C NMR spectrum (100 MHz, $CDCl_3$, 298K) of **2b**.

The proton NMR spectrum of **2** is shown in Fig. S8. ^{1}H NMR (400 MHz, $CDCl_3$, 298K) δ (ppm): 7.60 (s, 2H), 6.92 (d, J = 8 Hz, 4H), 8.84 (d, J = 8 Hz, 4H), 5.16 (s, 4H), 4.43 (t, J = 12 Hz, 4H), 3.90 (t, J = 8 Hz, 4H), 2.41 (t, J = 8 Hz, 4H), 2.11–2.08 (m, 4H), 1.77–1.63 (m, 9H), 1.45–1.32 (m, 14H). The ^{13}C NMR spectrum of **2** is shown in Fig. S9. The ^{13}C NMR (100 MHz, $CDCl_3$, 298K) δ (ppm): 153.79, 152.16, 144.89, 122.53, 118.91, 115.81, 115.41, 68.57, 62.73, 49.24, 29.48, 29.36, 29.06, 26.04, 22.32, 16.71.

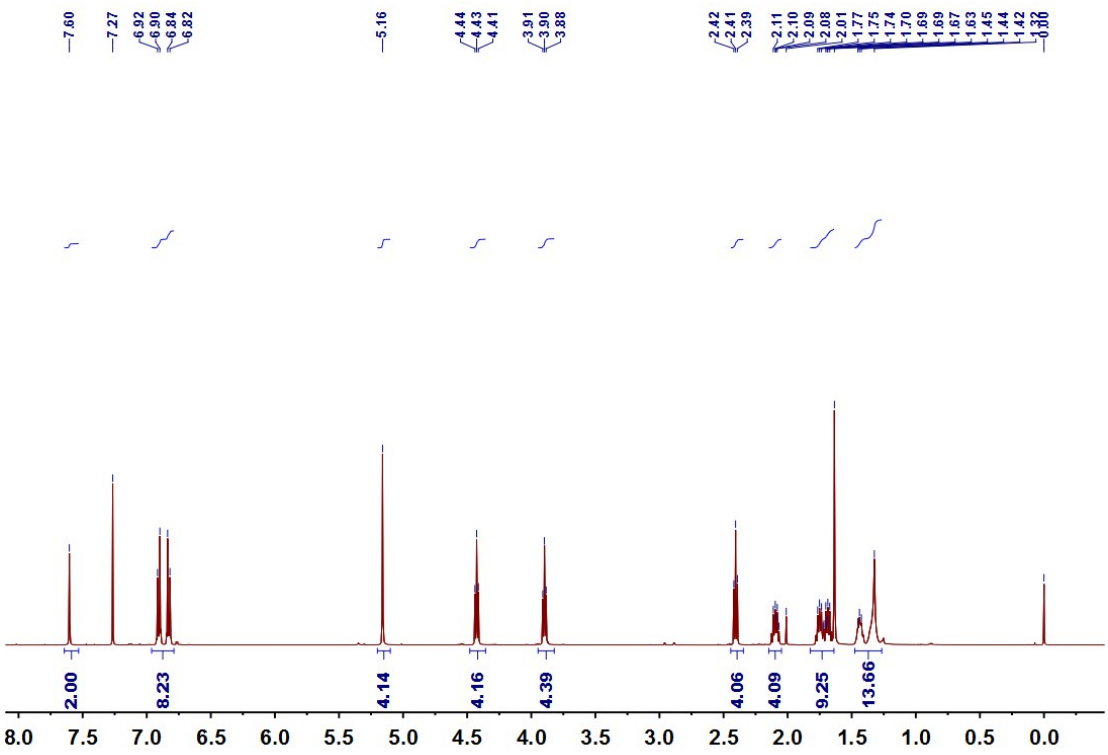

Fig. S8 ^{1}H NMR spectrum (400 MHz, $CDCl_3$, 298K) of **2**.

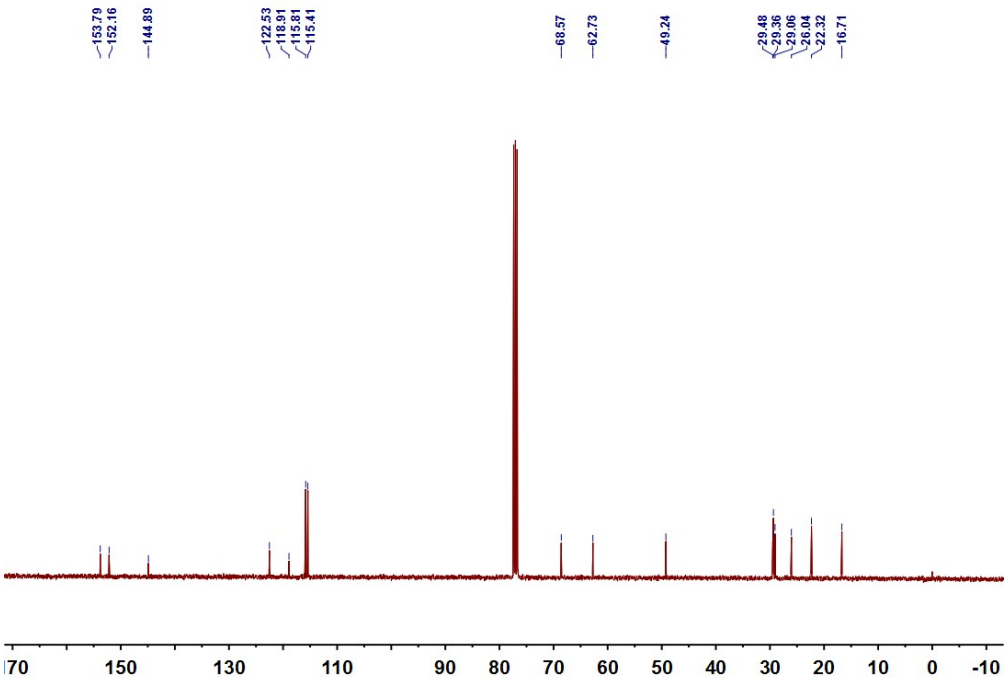

Fig. S9 ^{13}C NMR spectrum (100 MHz, $CDCl_3$, 298K) of **2**.

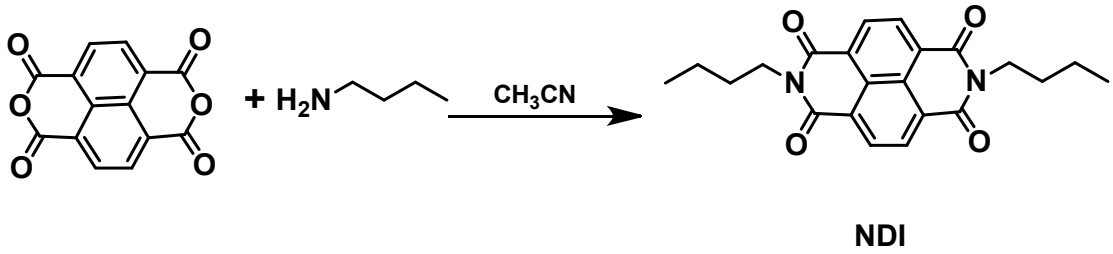

NDI

Scheme S3 *Synthetic route to* ***NDI***.

In a 250 mL round–bottom flask, 1, 4, 5, 8-Naphthalenetetracarboxylic dianhydride (2.50 g, 9.32 mmol), 1-Butanamine (5.45 g, 74.51 mmol) and acetonitrile (150 ml) were added. The reaction mixture was stirred at reflux for 48 hours. After the solid was filtered off, the solvent was removed and the residue was recrystallized from acetonitrile to give a red solid (1.38 g, 39.0%). The proton NMR spectrum of **NDI** is shown in Fig. S10. ^{1}H NMR (400 MHz, $CDCl_3$, 298K) δ (ppm): 8.75 (s, 4H), 4.21 (t, J = 16 Hz, 4H), 1.77–1.70 (m, 4H), 1.49–1.44 (m, 4H), 0.99 (t, J = 12 Hz, 6H). The ^{13}C NMR spectrum of **NDI** is shown in Fig. S11. The ^{13}C NMR (100 MHz, $CDCl_3$, 298K) δ (ppm): 161.75, 129.85, 125.57, 125.54, 39.70, 29.11, 19.30, 12.78.

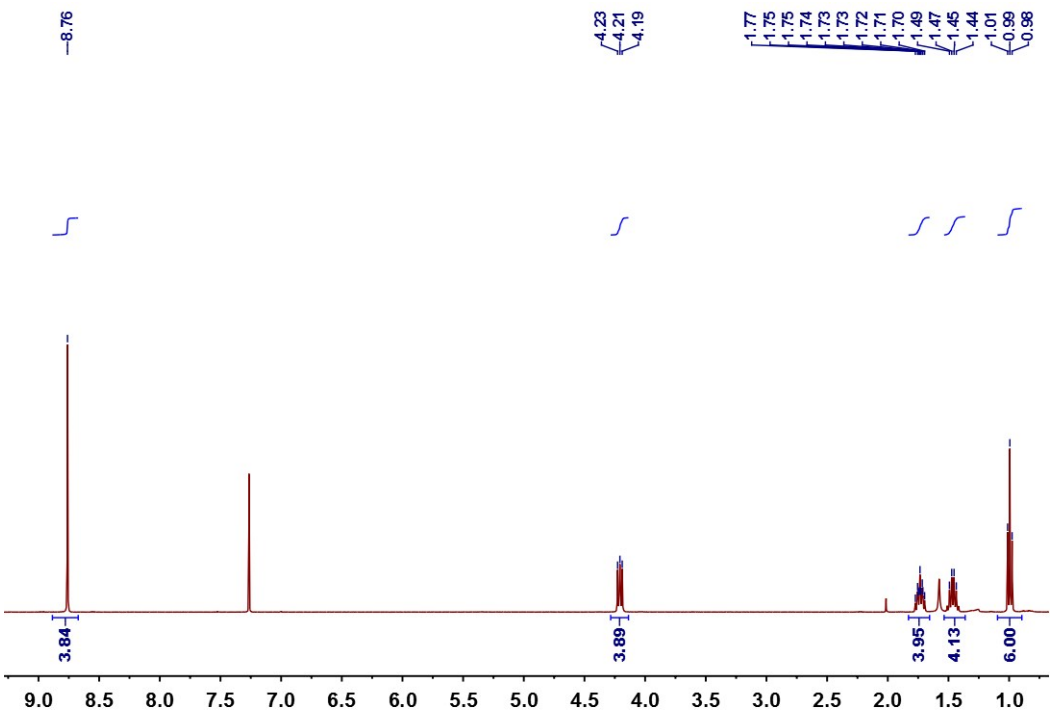

Fig. S10 ^{1}H NMR spectrum (400 MHz, $CDCl_3$, 298K) of **NDI**.

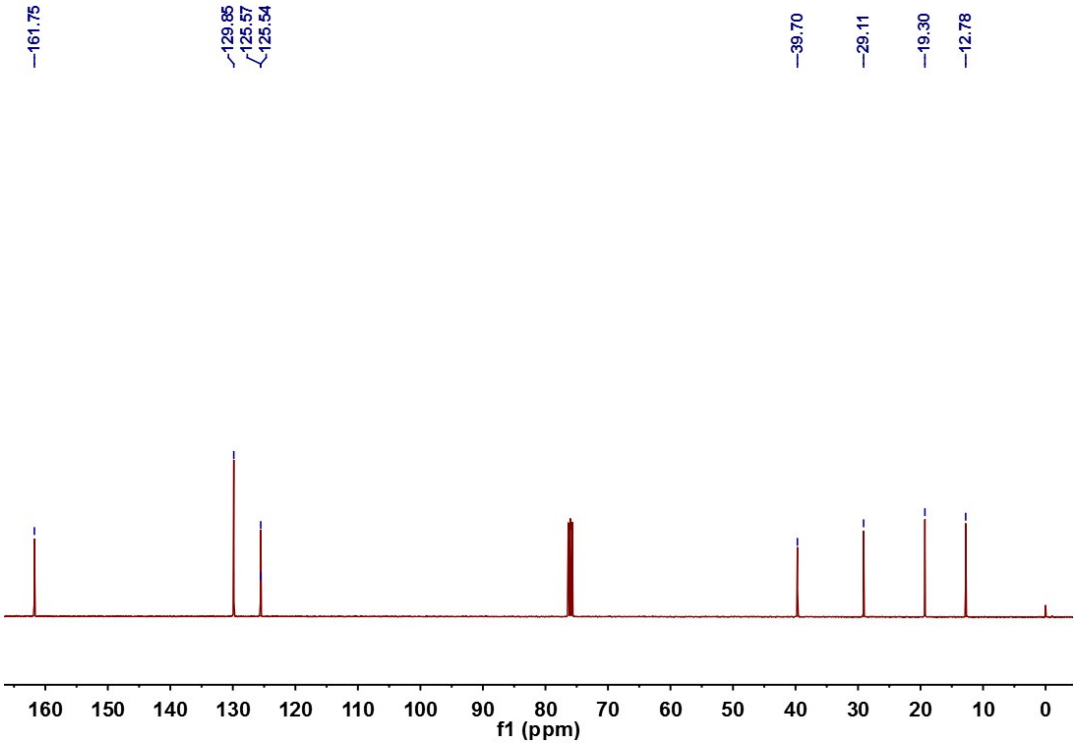

Fig. S11 ^{13}C NMR spectrum (100Hz, $CDCl_3$, 298K) of **NDI**.

*3 Absorbance spectra of **1**, **NDI** and **1**$_2$·**NDI***

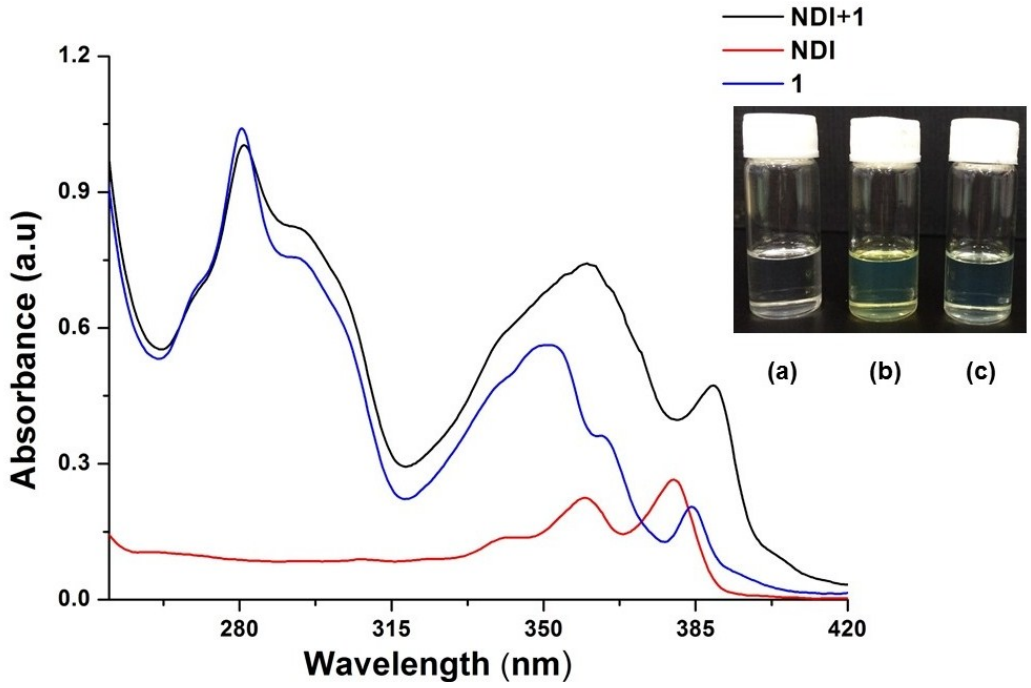

Fig S12 Absorbance spectra of **NDI** upon complexation with 2.0 equiv. of **1** (1.0×10^{-5} M) in $CHCl_3$. Inset: photographs show the colour of (a) **NDI**; (b) **1** + **NDI**; (c) **1**.

*4. Fluorescence spectra of **1**, **NDI** and **1**$_2$·**NDI***

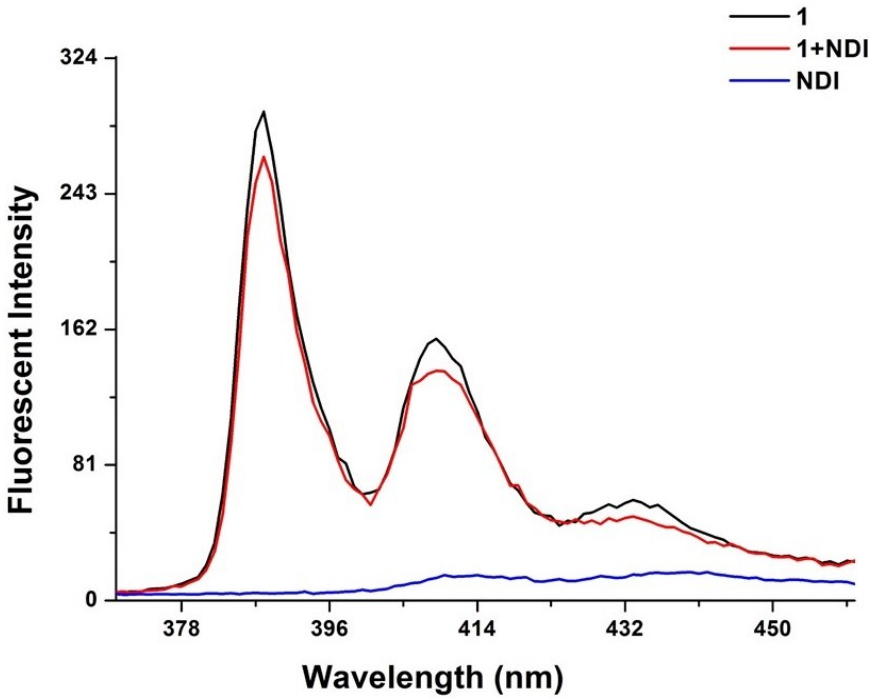

Fig S13 Fluorescence spectra of **NDI** upon complexation with 2.0 equiv. of **1** (1.0×10^{-6} M) in $CHCl_3$.

*5. ^{1}H NMR spectra of **NDI** in the absence and presence of host **1***

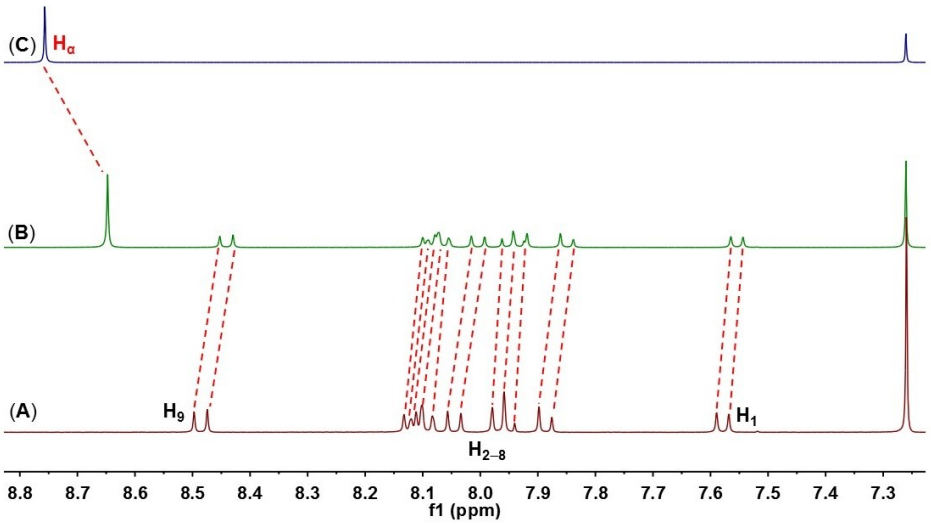

Fig S14 Partial ^{1}H NMR spectra (400 MHz, $CDCl_3$, 298K) of **NDI** upon complexation with 2.0 equiv. of **1** (10 mM). (A) **1**; (B) **1** + **NDI**; (C) **NDI**.

*6. ^{1}H NMR spectra of guest **2** in the absence and presence of host **1***

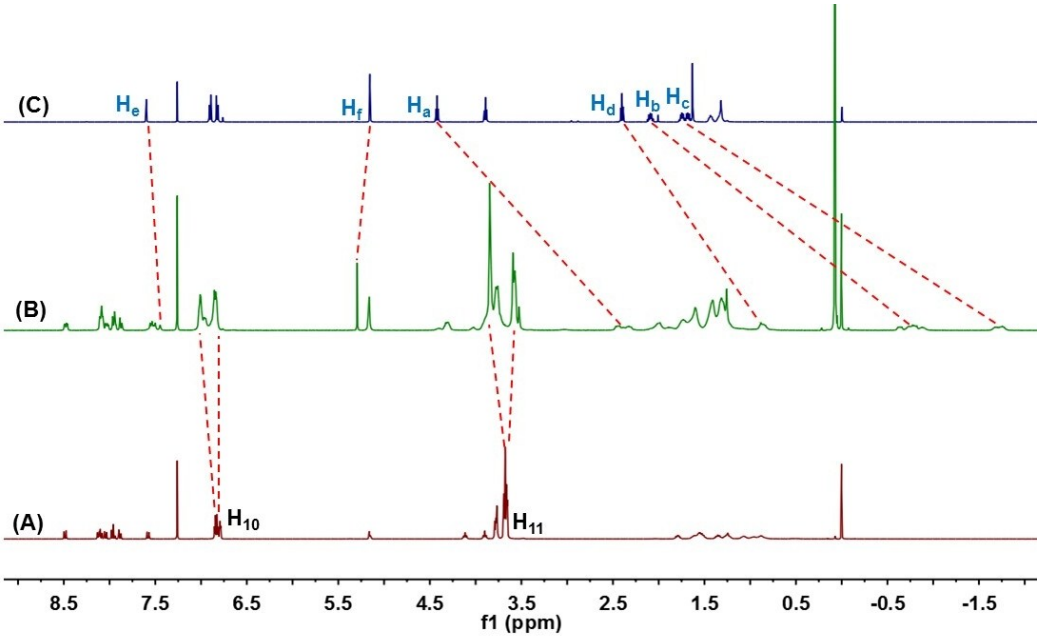

Fig S15 ^{1}H NMR spectra (400 MHz, $CDCl_3$, 298K) of **2** upon complexation with 2.0 equiv. of **1** (10 mM). (A) **1**; (B) **1** + **2**; (C) **2**.

7. NOESY NMR spectrum of ***1***$_2$***·2***

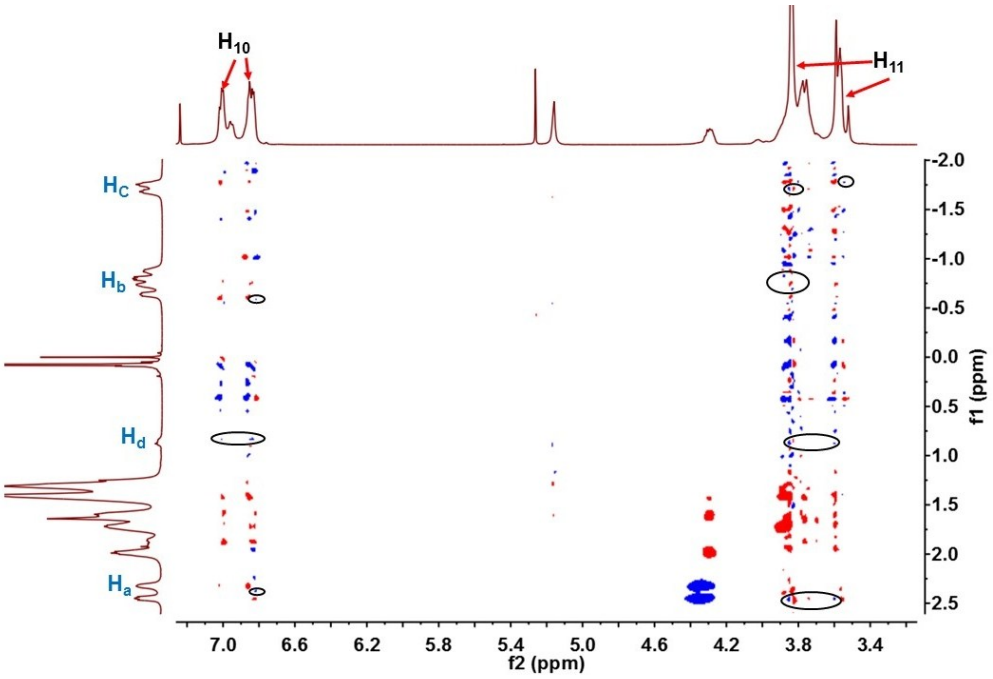

Fig S16 Partial NOESY NMR spectrum (500 MHz, $CDCl_3$, 298K) of **1**$_2$**·2** at the concentration of 10 mM.

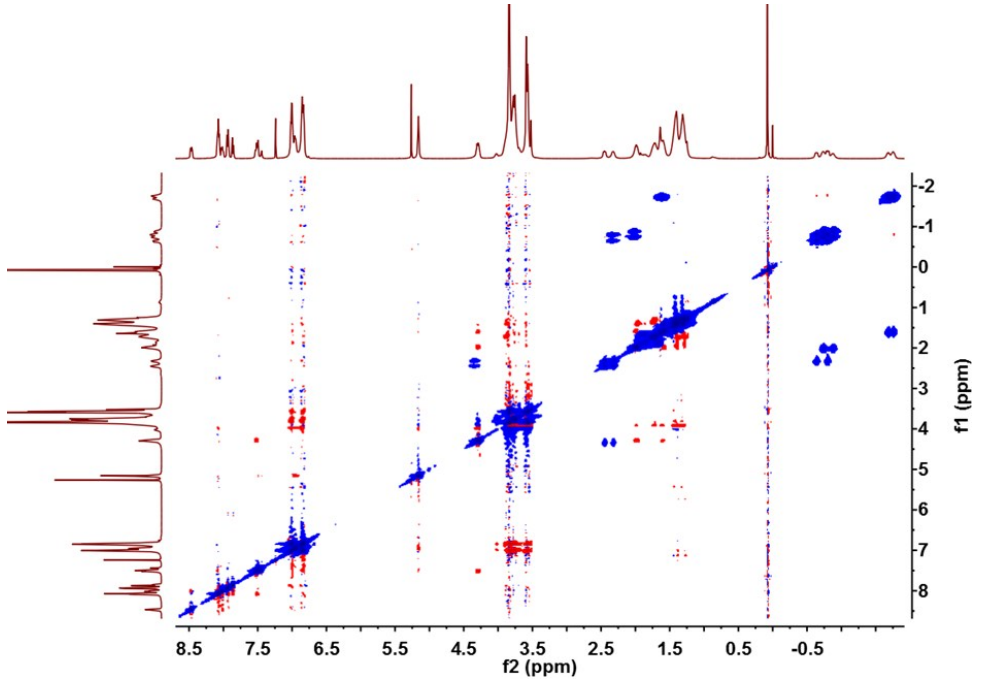

Fig S17 NOESY NMR spectrum (500 MHz, $CDCl_3$, 298K) of **1**$_2$**·2** at the concentration of 10 mM.

*8. Partial ^{1}H NMR spectra of **1_2·NDI·2** at different concentrations*

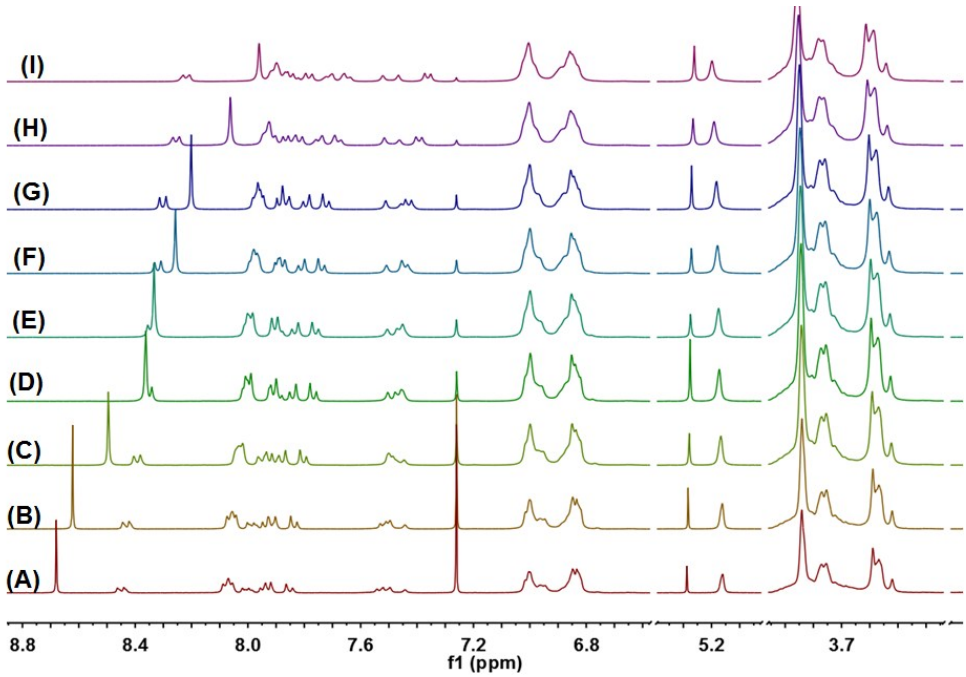

Fig. S18 Partial ^{1}H NMR spectra (400 MHz, 298 K) of **1_2·NDI·2** in $CDCl_3$ at various concentrations: (A) 5.00 mM; (B) 10.0 mM; (C) 25.0 mM; (D) 50.0 mM; (E) 62.5 mM; (F) 76.5 mM; (G) 100 mM; (H) 140 mM; (I) 200 mM.

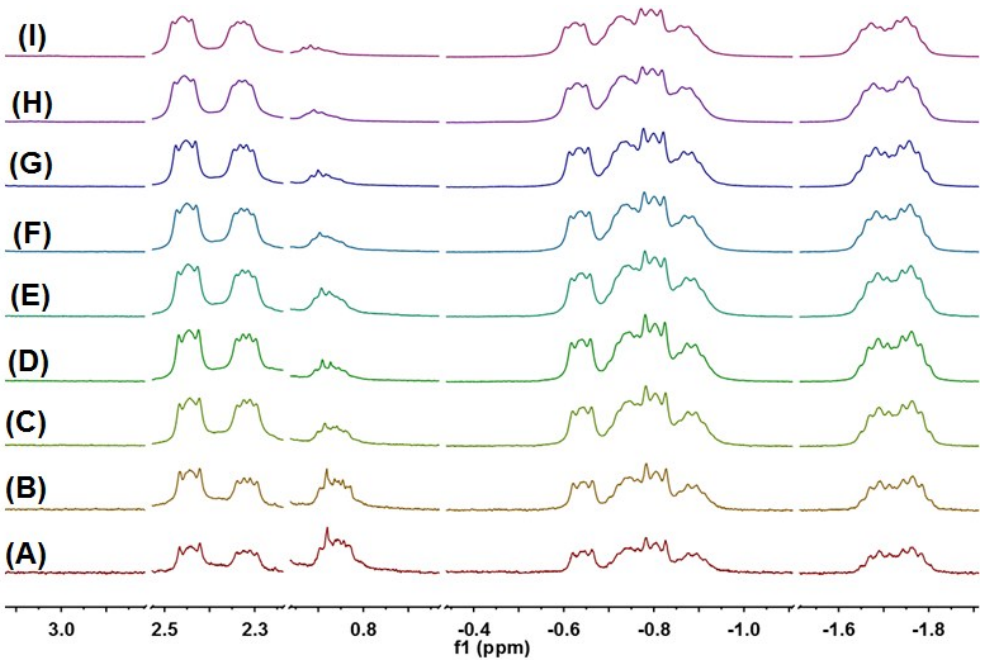

Fig. S19 Partial ^{1}H NMR spectra (400 MHz, 298 K) of **1_2·NDI·2** in $CDCl_3$ at various concentrations: (A) 5.00 mM; (B) 10.0 mM; (C) 25.0 mM; (D) 50.0 mM; (E) 62.5 mM; (F) 76.5 mM; (G) 100 mM; (H) 140 mM; (I) 200 mM.

9. Determination of diffusion coefficient D

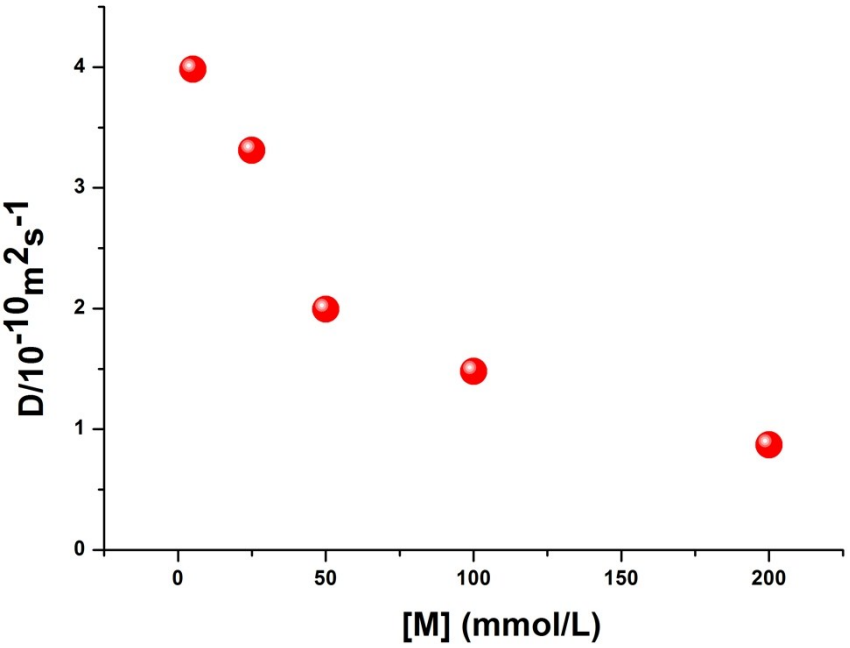

Fig. S20 Concentration dependence of diffusion coefficient *D* (500 MHz, $CDCl_3$, 298K).

10. Calculated values of maximum polymerization degree n at different concentrations of ***1_2·NDI·2***

Using the Carothers equation[S3] and assuming that the same average association constant holds for each successive step (isodesmic) and that cyclic species can either be ignored or taken into account, the average degree of polymerization, *n*, is easily derived as being related to the equilibrium constant K_a and the initial monomer concentration as follows:[S4]

If we now define *p* = extent of complexation,

$K_a = p[H]_0/(1 - p)^2[H]_0^2$.

Solving this quadratic equation leads to

$1 - p = \{(1 + 4K_a[H]_0)^{1/2} - 1\}/2K_a[H]_0$

$n = 1/(1 - p) = 2K_a[H]_0/\{(1 + 4K_a[H]_0)^{1/2} - 1\}$ (1)

if $4K_a[H]_0 \gg 1$, $n = 2K_a[H]_0/\{(4K_a[H]_0)^{1/2} - 1\}$ and

if $(4K_a[H]_0)^{1/2} \gg 1$, $n = (K_a[H]_0)^{1/2}$ (2)

The marriage of donor–acceptor interactions and host–guest recognition provides a

facile strategy for getting monomeric unit $\mathbf{1}_2$·**NDI**·**2**. The component $\mathbf{1}_2$·**NDI** may be thought of as an unusual homoditopic AA-type monomer ($\mathbf{1}_2$), and a neutral guest **2** was used as a BB-type monomer.

In this system p is the extent of complexation and $[H]_0 = [\mathbf{1}_2\cdot\mathbf{NDI}\cdot\mathbf{2}]_0 = [\mathbf{1}]_0 = 2([\mathbf{2}]_0)$. Therefore, degrees of polymerization calculated in this way represent maximum values that in practice will be reduced by formation of cyclics and possibly by reduction in the association constant as the suprapolymer grows ("attenuation"). As the concentration increases, the calculated size of aggregates increases to large values. Here the association constant (K_a) values of model systems MeP5A⊃TAPN was used in the calculations with Eqs. 1 and 2.

Table S1. Calculated values of p and n at different concentrations of $\mathbf{1}_2$·**NDI**·**2**

$(\mathbf{1}_2\cdot\mathbf{NDI}\cdot\mathbf{2})_0$ (mM)	p	max n
0.500	0.675	3.08
15.0	0.928	13.9
60.0	0.963	27.3
100	0.972	35.1
142	0.976	41.8
250	0.982	55.3

11. Variable temperature partial ^{1}H NMR spectra of ***1_2·NDI·2***

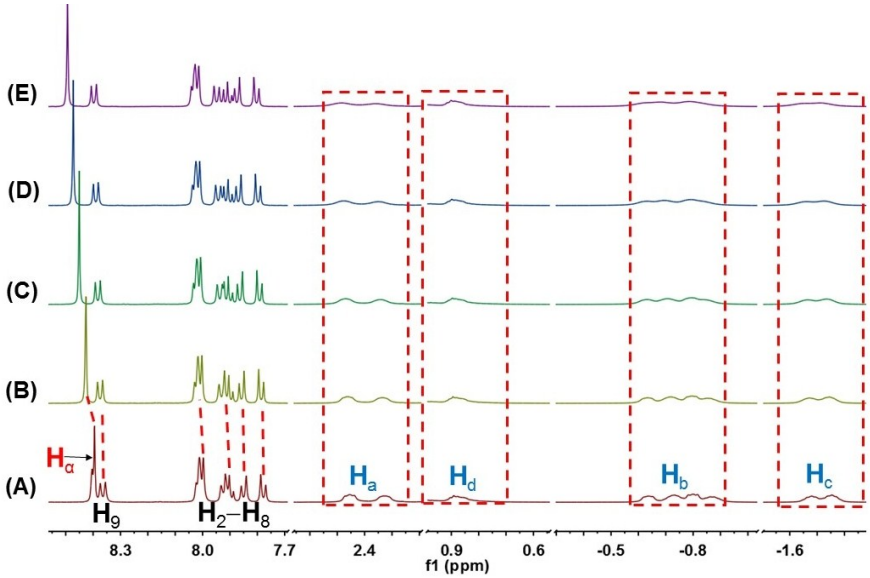

Fig. S21 Variable temperature partial ^{1}H NMR spectra of **1_2·NDI·2** (150 mM, $CDCl_3$, 500 MHz): (A) 298 K; (B) 303 K; (C) 308 K; (D) 313 K and (E) 318 K.

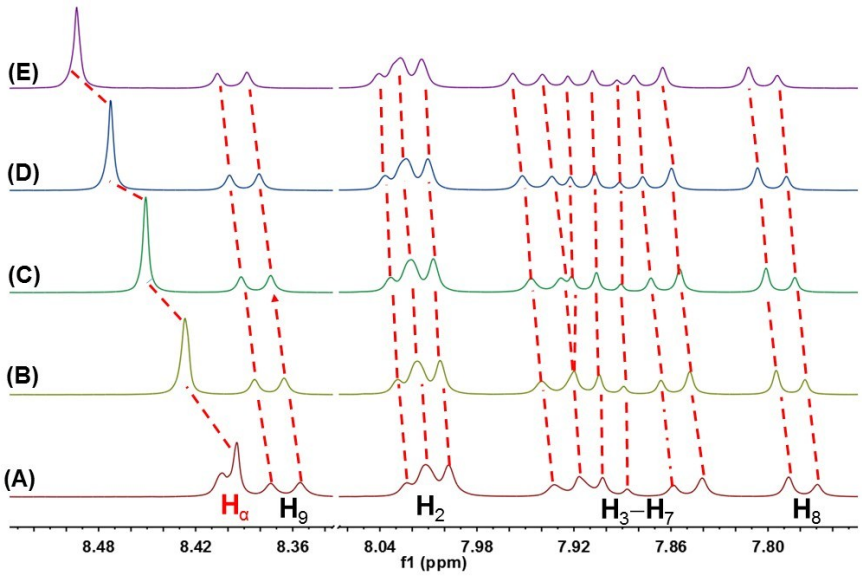

Fig. S22 Enlarged image of Figure S21 from 8.53 ppm to 7.76 ppm.

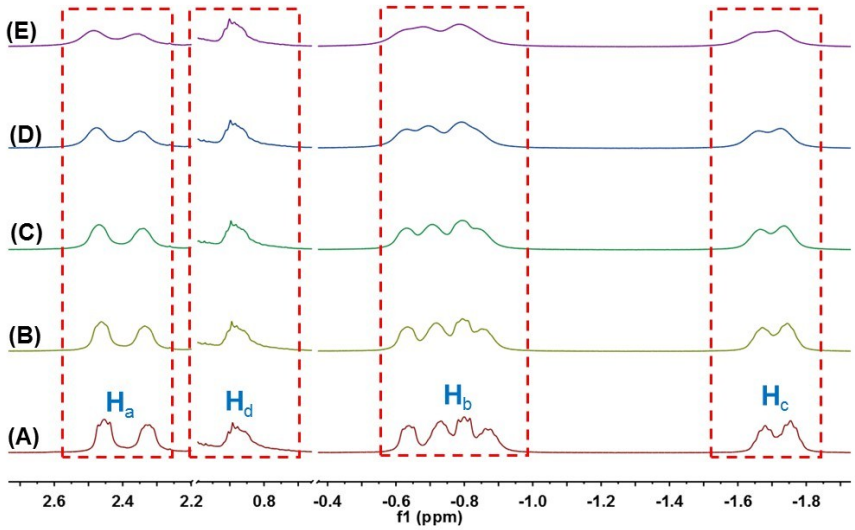

Fig. S23 Enlarged image of Figure S21 from 2.56 ppm to −1.85 ppm.

12. References

1. Z. Zhang, G. Yu, C. Han, J. Liu, X Ding, Y. Yu and F. Huang, *Org. Lett.*, 2011, **13**, 4818.
2. C. Li, K. Han, J. Li, Y. Zhang, W. Chen, Y. Yu and X. Jia, *Chem. Eur. J.*, 2013, **19**, 11892.
3. C. H. Carothers, *Trans. Faraday Soc*., 1936, **32**, 39.
4. (*a*) H. W. Gibson, N. Yamaguchi and J. W. Jones, *J. Am. Chem. Soc*., 2003, **125**, 3522; (*b*) F. Huang, D. S. Nagvekar, X. Zhou and H. W. Gibson, *Macromolecules*, 2007, **40**, 3561: (*c*) B. Xia, B. Zheng, C. Han, S. Dong, M. Zhang, B. Hu, Y. Yu and F. Huang, *Polym. Chem*., 2013, **4**, 2019.